PAPER

Check for updates

A novel modified nano-alumina composite sol for potential application in forest firefighting

Weining Du, [ID] Mingqiang Yan, Chaolu Yin* and Zejiang Zhang

Herein, modified ammonium polyphosphate wrapped nano-alumina (mAPP@Als) was first synthesized and then dispersed in traditional fire extinguishing solution (FES) to fabricate a FES-mAPP@Als composite sol. It was found that the phosphorus-silica containing units were attached onto the nano-alumina surface, and the mAPP@Als particles showed excellent dispersion level in FES with a single-domain particle size distribution range. Due to the synergistic effects of the phosphorus–nitrogen and silica–alumina flame retardant components, FES-mAPP@Als (5% concentration) coated wood exhibited improved limiting oxygen index (33.2%) and carbonization ability, and depressed heat release (41.9%) and smoke production (10.7%), as compared to the pristine wood. In addition, the FES-mAPP@Als composite sol showed enhanced fire-extinguishing and anti-reignition capacities compared to the FES. This research offers a novel composite sol fire extinguishing agent for fighting forest fires.

1. Introduction

Forest fires are one of the most serious worldwide disasters in nature, and are a great threat to the ecological environment, human health, and animal lives.[1–3] Water is the commonly used extinguishing agent, due to the good cooling effect under fire, however, the fire extinguishing efficiency of water alone is poor when facing large-area forest fires.[4,5] The previous literature reported that addition of soluble chemical additives (surfactant and phosphorus–nitrogen active salts) could remarkably improve the fire-fighting performance, owing to the improved wetting, penetrating, and active free radical quenching ability surrounded the surface fuels.[6,7] Nevertheless, such extinguishing agents cannot form a compact carbonaceous protective layer on the solid fuel substrates, which limits their fire suppression efficiency.

To overcome these problems, various nano-particles such as silica, silver, alumina, and so on have been proposed for fire-fighting and fire prevention.[8–14] Pries *et al.*[8] claimed that silica sol can penetrate and preserve in the surface and pores of wood, and thus is favorable to target fire resistance. However, the used raw materials of silica sol were expensive, which limited the largescale application. Mosina *et al.*[12] reported alumina sol can form protective layer on the wood surface, which has good heat resistance, insulating, and environmental-friendly properties. Nevertheless, the combustion parameters (*i.e.*, limiting oxygen index, heat, smoke release, and so on) of the alumina-based sol on the wood substrate were not mentioned. Additionally, the firefighting and fire prevention efficiency of the single alumina

sol was still limited. Incorporation of alumina sol into phosphorus–nitrogen containing salts solutions is one of the simple and efficient way to significantly improve the target fire extinguishing efficiency. Nevertheless, the dispersion level of pristine alumina sol in the basic salts solutions is poor.

Ammonium polyphosphate (APP) has been widely used as acid and blowing sources in intumescent flame-retardant system, due to its merits of halogen-free, low toxicity, and high flame-retardant efficiency.[15–17] Its efficiency is generally assigned to the capture of free radicals in gas phase and increase the char formation in condensed phase.[18,19] According to the previous literature,[20,21] it is envisaged that modified alumina sol with APP or its derivatives might effectively improve its flame-retardant ability. It is also conducive to improve the dispersibility of modified alumina sol in basic salts solutions.

In this work, we first synthesized modified ammonium polyphosphate wrapped nano-alumina (mAPP@Als), and thus dispersed it into basic fire extinguishing solution (FES) to fabricate FES-mAPP@Als composite sol. The structure of mAPP@Als particles and its dispersion level in FES were characterized. Moreover, combustion behaviors such as limiting oxygen index, heat release, smoke production of FES-mAPP@Als coated wood, and the structures of char residue were systematically studied. The active firefighting efficiency of FES-mAPP@Als was further proposed and discussed.

2. Experimental

2.1. Materials

Ammonium chloride, carbamide, diammonium hydrogen phosphates, polyoxyethylene lauryl ether, aqueous ammonia, aluminium chloride, nitric acid, acetic acid, and polyethylene

Sichuan Fire Research Institute of Ministry of Emergency Management, Chengdu 610036, China. E-mail: yinchaolu@scfri.cn

glycol (PEG-400) were purchased from Sichuan Shudu Chemical Reagent Co., Ltd (Chengdu, China). Ammonium polyphosphate, (3-aminopropyl)trimethoxysilane, and anhydrous ethanol were provided by Chengdu Huaxia Chemical Reagent Co., Ltd (Chengdu, China). The above chemicals were used as received without further purification. Deionized water was prepared in our laboratory.

2.2. Preparation of modified nano-alumina composite sol

Modified nano-alumina composite sol was prepared through a three-step method.

In the first step, 2 L of aqueous ammonia (1 mol L^{-1}) was put into a flask, then 100 mL of aluminium chloride solution (2 mol L^{-1}) and 10 g of polyethylene glycol were added to the above solution with a dripping speed of 10 mL min^{-1}, and stirred at 90 °C for 2 h. After further ageing 5 h, the mixture was centrifuged and washed with deionized water at least five times. The obtained solid product was redispersed in 1 L of deionized water, and 80 mL of nitric acid solution (0.5 mol L^{-1}) was added to the solution under a high-speed stirring (2000 rpm). Finally, the nano-alumina sol was achieved, and abbreviated as Als.

In the second step, 10 g of ammonium polyphosphate (APP) and 1 g of (3-aminopropyl)trimethoxysilane were completely dispersed in 50 mL of anhydrous ethanol, and stirred at 80 °C for 8 h. The modified APP was achieved by ultracentrifugation method, and labeled as mAPP. The equal amount of mAPP and Als samples were dispersed in a water/ethanol solution, and the

pH value of the above mixture was adjusted to about 3.5 with acetic acid, and further maintained at 60 °C for 6 h. The mixture was purified under a reduced pressure (0.09 MPa), the obtained mAPP modified Als sol was coded as mAPP@Als.

In the third step, the control fire extinguishing solution (FES) consisted of 180 g ammonium chloride, 300 g carbamide, 500 g diammonium hydrogen phosphates, 20 g polyoxyethylene lauryl ether, and 19 L water. In case of same concentration of 5%, the equal amount of Als (or mAPP@Als sol) and FES solution were completely mixed with a mechanically stirring, the acquired composite sol was labeled as FES-Als (or FES-mAPP@Als).

2.3. Characterization

Fourier transform infrared (FT-IR) was measured on a Nicolet-iS10 FTIR Spectrometer (Thermo Scientific, USA). Each sample was recorded in the wavenumber range of 500–4000 cm^{-1} with a resolution of 4 cm^{-1}. Thermo-gravimetric (TG) analysis was conducted on a TG-209 (Netzsch, Germany) under nitrogen atmosphere. Each sample was heated from 50 to 600 °C at a rate of 20 K min^{-1}. The particle size distribution of prepared dispersions (0.1 mg mL^{-1}) were determined using a Nano-ZS90 laser granulometer (Malvern, US) at room temperature. Transmission electron microscopy (TEM) was performed by using an HT-7800 microscope (Hitachi, Japan) at 80 kV. Each sample was diluted in aqueous solution, and subsequently coated on a copper grid of 200 mesh. Combustion behavior was measured on a cone calorimeter (FTT, UK). Each sample with a square
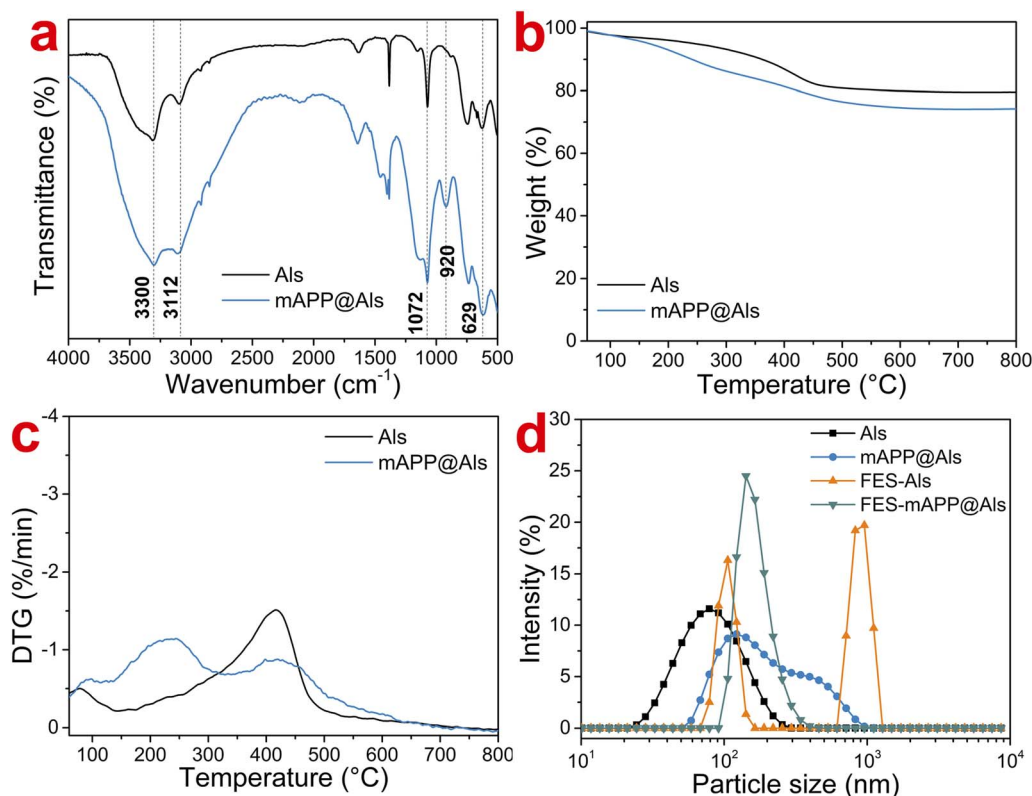

Fig. 1 (a) FTIR, (b) TG, and (c) DTG curves of powdery Als and mAPP@Als; (d) particle size distribution of Als, mAPP@Als, FES-Als, FES-mAPP@Als dispersions.
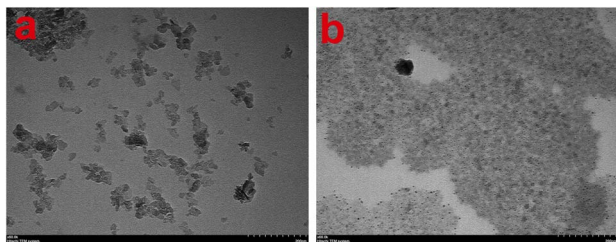
Fig. 2 Representative TEM images of (a) Als and (b) mAPP@Als.

microscope (FEI, USA) at 15 kV. Raman spectroscopy (RM) was carried out using an inVia Reflex confocal Raman microscope (Renishaw, UK) at 532 nm in the range of 500–2000 cm^{-1}. For the fire extinguishing experiment, the prepared sample was put into a stored pressure fire extinguisher (6 L, 1.2 MPa). The square wood crib with a dimension of 500 mm was ignited by heptane, and burned absolutely for 5 min, and thus extinguished by the self-made fire extinguisher.

shape (100 mm × 100 mm × 5 mm) was estimated according to the ISO 5660 standard method under a flux of 35 kW m^{-2}. Limiting oxygen index (LOI) was determined using a HC-2C oxygen index meter (Ascent, China) in terms of the ASTM D-2863 standard method. Scanning electron microscopy (SEM) was performed on a Apreo S HiVoc scanning electron

3. Results and discussion

Fig. 1a shows the FTIR curves of Als and mAPP@Als. It could be seen that both Als and mAPP@Als possessed characteristic peaks at 3112–3300 cm^{-1} (stretching vibration of O–H), 1072 cm^{-1} (symmetric- and asymmetric-stretching vibrations of Al–O–H), and 629 cm^{-1} (bending vibration of Al–O), suggesting the fundamental structure of alumina hydrosol.[22–24] Notably,

Table 1 Combustion results including LOI (limiting oxygen index), TTI (time to ignition), PHRR (maximum peak heat release rate), T_{PHRR} (time of maximum peak heat release rate), THR (total heat release), TSP (total smoke production), and char residue of the W, W-FES, and W-FES-mAPP@Als

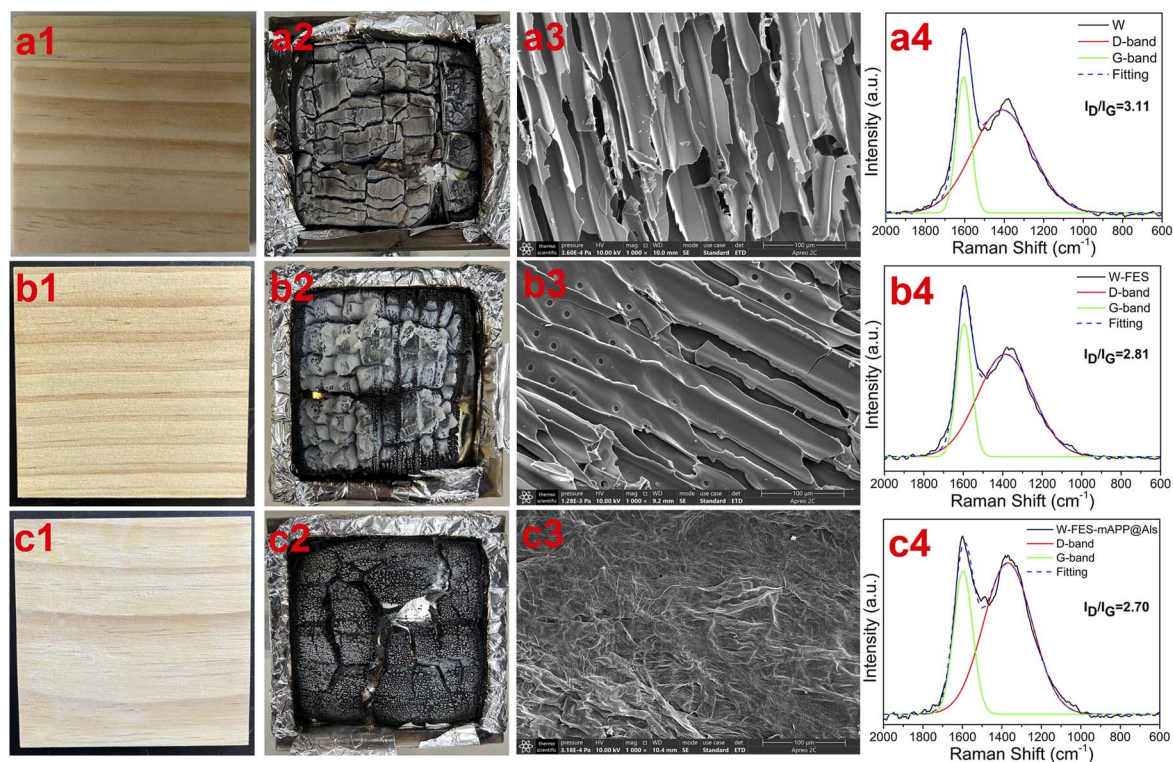| Sample	LOI (%)	TTI (s)	PHRR (kW m^{-2})	T_{PHRR} (s)	THR (MJ m^{-2})	TSP (m^2)	Char residue (%)
W	25.1	35	172.3	360	48.7	12.1	14.8
W-FES	30.1	262	190.0	310	36.0	12.7	17.5
W-FES-mAPP@Als	33.2	316	150.8	385	28.3	10.8	19.0

Fig. 3 Images of W, W-FES, W-FES-mAPP@Als samples (a1–c1) before and (a2–c2) after cone calorimeter experiment; the corresponding (a3–c3) SEM micrographs and (a4–c4) Raman curves of the char residues after combustion.

© 2023 The Author(s). Published by the Royal Society of Chemistry

mAPP@Als exhibited broader peaks at around 3200 cm^{-1} and 1000–1100 cm^{-1} than that of Als, which assigned to the N–H and Si–O–Si (or P–O) stretching vibrations, respectively.[17] Additionally, a new peak at 920 cm^{-1} (stretching vibration of Si–O–Al) appeared in mAPP@Als.[25] These results indicated the mAPP unit was covalently attached on the surface of Als.

Fig. 1b and c display the TG and DTG curves of Als and mAPP@Als, respectively. It could be found that mAPP@Als showed higher weight loss than the Als over the whole temperature range, and the residue weights for Als and mAPP@Als were 79.5% and 74.2%, respectively. Moreover, the main decomposition region for Als was seen at 200–500 °C, whereas mAPP@Als possessed two decomposition regions of 150–350 °C and 350–600 °C. The results indirectly suggested the presence of mAPP unit on the mAPP@Als surface, and the P- and Si-containing compound could contribute to its thermally stable at high temperature.

Fig. 1d presents the particle size distribution of Als, mAPP@Als, FES-Als, FES-mAPP@Als dispersions. As observed from Fig. 1d, Als and mAPP@Als possessed single-domain particle size distribution ranges, and their average particle sizes were 70.0 nm and 229.3 nm, respectively. The increment of average particle size for mAPP@Als might be due to the wrapped mAPP on the mAPP@Als surface. After blending with FES, the FES-Als transformed into two-domain particle size distribution range, and the average particle size increased to 713.4 nm, owing to the flocculation effect of Als in basic FES solution. By contrast, the particle size distribution range and average particle size for FES-mAPP@Als (223.0 nm) were comparable to the mAPP@Als, indicating the good dispersibility and stability of mAPP@Als particles in FES. The microstructure and dispersion level of Als and mAPP@Als were further recorded by TEM, as shown in Fig. 2. It could be seen that large amounts of Als particles aggregated together into clusters with different degree. By contrast to the Als, the mAPP@Als showed a relatively smaller particle size and uniform spherical shape. Moreover, the mAPP@Als particles exhibited better dispersibility than that of Als, mainly due to the attached mAPP unit. The high dispersion level and nano-size of the mAPP@Als particles in the FES might synergistically improve the permeability on wood surface, and thus contribute to the fire extinguishing efficiency.

Because the neat Als had poor dispersion level in FES, thus the FES and FES-mAPP@Als were used to study the fire prevention behavior on wood substrate (Table 1). Clearly, the untreated W possessed lower LOI (25.1%), TTI (35 s), T_{PHRR} (360 s), char residue (14.8%) values, and higher PHRR (172.3 kW
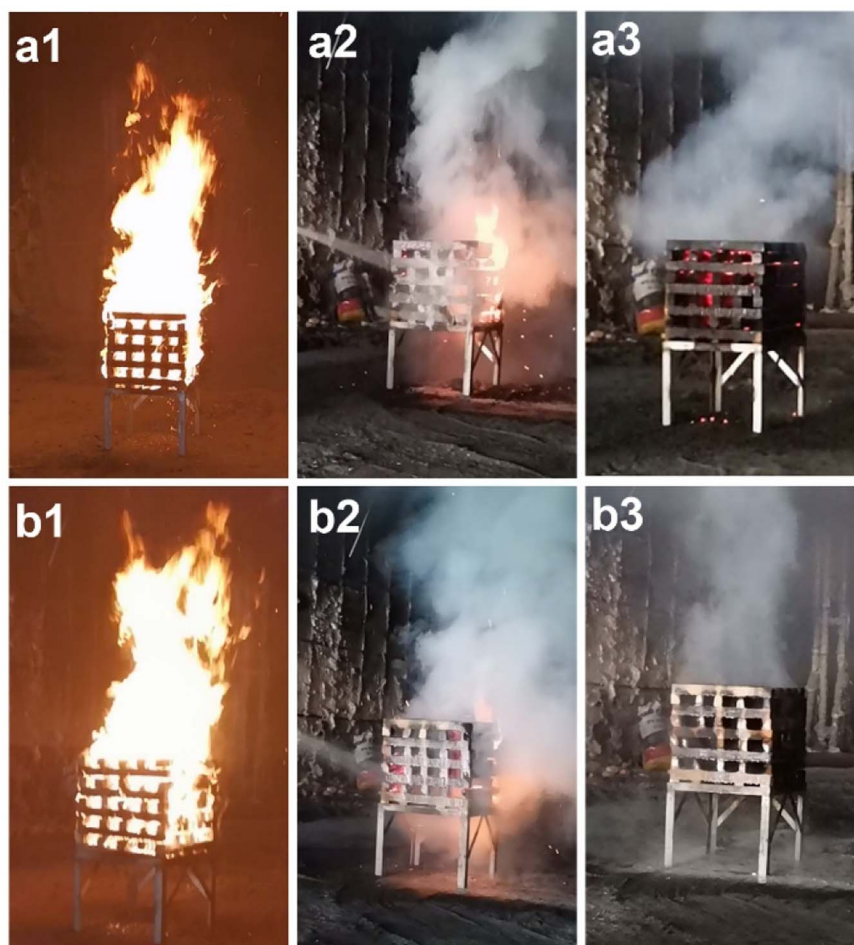

Fig. 4   Fire extinguishing process of (a1–a3) FES and (b1–b3) FES-mAPP@Als with a 6 L fire extinguisher.

m^{-2}), THR (48.7 MJ m^{-2}), TSP (12.1 m^2) values except for the W-FES. In comparison with W, the LOI, TTI, and char residue values for W-FES and W-FES-mAPP@Als were improved, while the corresponding THR value was reduced. Unfortunately, W-FES exhibited higher PHRR and TSP values, and earlier T_{PHRR} than that of W. This result might be that the FES coated wood cannot form compact carbonaceous char under fire, resulting in higher heat and smoke release. In comparison with W-FES, the W-FES-mAPP@Als possessed relative higher LOI (33.2%), TTI (316 s), T_{PHRR} (385 s), char residue (19.0%) values, and lower values of PHRR (150.8 kW m^{-2}), THR (28.3 MJ m^{-2}) and TSP (10.8 m^2) values. Such phenomenon could be explained by the synergistic flame retardancy effects of the phosphorus–nitrogen and silica–aluminium units in FES-mAPP@Als coated wood.

Fig. 3(a1–c1) and (a2–c2) show the digital images of W, W-FES, W-FES-mAPP@Als samples before and after cone calorimeter test, respectively. Obviously, the upper-surfaces of W and W-FES char residue were relative looser and adhered large amounts of ash. By contrast, the W-FES-mAPP@Als exhibited a denser carbonization block than those of W and W-FES. Fig. 3(a3–c3) showed that large amounts of pores and fragments appeared in W and W-FES char residues, due to the gases release and the structural collapse of the wood substrate during combustion. In contrast, the W-FES-mAPP@Als char residue showed non-pore and compact continuous surface, which capable of storing the gases in the char layer. Fig. 3(a4–c4) presents the Raman curves of the char residues. Notably, the W-FES-mAPP@Als char residue possessed the lowest values of I_D/I_G, indicating a better graphitization degree under fire. These results suggested the superior carbonization ability of W-FES-mAPP@Als during the combustion, leading to improved fire prevention.

Fig. 4 shows the fire extinguishing process of FES and FES-mAPP@Als. Both FES and FES-mAPP@Als samples could complete firefighting, and the fire-extinguishing times were 40 s and 30 s, respectively. However, the wood crib was reignited when the fire extinguisher containing FES consumed up. By contrast to the FES, the FES-mAPP@Als composite sol could more efficient and fast extinguishing the wood crib fire, and there was no smoldering fire after standing for 15 min. The possible fire-extinguishing mechanism for FES-mAPP@Als composite sol might be that the phosphorus- and nitrogen-containing units could quench the active oxygen and hydrogen free radicals and release noncombustible gases (*e.g.*, ammonia, nitrogen oxide, carbon dioxide, water vapor, and so on) under fire, and concurrently, the formed phosphorus acid and the existing silica–aluminium components could coordinately form strengthened carbonaceous protective layers on the wood substrate, leading to significantly improvement of fire suppression and anti-reignition capacities.

4. Conclusions

In summary, a typical FES-mAPP@Als composite sol was fabricated by blending the modified ammonium polyphosphate wrapped nano-alumina (mAPP@Als) and fire extinguishing solution (FES). The successful modification of mAPP@Als was verified by the FTIR and TG-DTG measurements. Dynamic light scattering result revealed that mAPP@Als particles could maintain a single-domain nanoscale particle size distribution range and admirable dispersion level in FES medium, and the average particle size was 223.0 nm. Notably, the 5% FES-mAPP@Als coated wood showed relative higher LOI (33.2%), TTI (316 s), T_{PHRR} (385 s), char residue (19.0%) values, and lower values of PHRR (150.8 kW m^{-2}), THR (28.3 MJ m^{-2}) and TSP (10.8 m^2) values among the experimental samples. In addition, FES-mAPP@Als composite sol could effectively extinguish the wood crib fire (30 s) and prevent reignition. The present research provides a promising way to fabricate nano-metal based composite sol with excellent fire extinguishing and prevention ability.

Conflicts of interest

There are no conflicts to declare.

Acknowledgements

References

1 C. Narayan, P. M. Fernandes, J. van Brusselen and A. Schuck, *For. Ecol. Manage.*, 2007, **251**, 164–173.

2 D. A. Hanson, E. M. Britney, C. J. Earle and T. G. Stewart, *For. Ecol. Manage.*, 2013, **294**, 166–177.

3 X. Guan, Y. Wei, K. Liu and S. Q. Shi, *Alexandria Eng. J.*, 2020, **59**, 2233–2238.

4 R. Hansen, *Int. J. Wildland Fire*, 2012, **21**, 525–536.

5 J. Rakowska, R. Szczygieł, M. Kwiatkowski, B. Porycka, K. Radwan and K. Prochaska, *Fire Technol.*, 2017, **53**, 1379–1398.

6 H. Hybská, L. M. Osvaldová, M. Horváthová, T. Hýrošová and Á. Restás, *BioResources*, 2022, **17**, 1988–2002.

7 G. V. Kuznetsov, A. G. Islamova, E. G. Orlova, P. A. Strizhak and D. V. Feoktistov, *Fire Saf. J.*, 2021, **123**, 103371.

8 M. Pries and C. Mai, *Eur. J. Wood Wood Prod.*, 2013, **71**, 237–244.

9 L. P. Yu, M. F. Tian, L. F. Li, Z. G. Wu, S. C. Chen, J. Chen and X. D. Xu, *Wood Res.*, 2020, **65**, 797–808.

10 L. A. Lowden and T. R. Hull, *Fire Sci. Rev.*, 2013, **2**, 4–23.

11 L. Zhang, S. Shu and Y. Bian, *Thermochim. Acta*, 2022, **718**, 179389.

12 K. S. Mosina, E. A. Nazarova, A. V. Vinogradov, V. V. Vinogradov and P. V. Krivoshapkin, *ACS Appl. Nano Mater.*, 2020, **3**, 4386–4393.

13 J. Mastalska-Popławska, Ł. Wójcik and P. Izak, *J. Sol-Gel Sci. Technol.*, 2023, **105**, 608–624.

14 A. Rabajczyk, M. Zielecka and J. Gniazdowska, *Materials*, 2022, **15**, 8876.

15 K. S. Lim, S. T. Bee, L. T. Sin, T. T. Tee, C. T. Ratnam, D. Hui and A. R. Rahmat, *Composites, Part B*, 2016, **84**, 155–174.

16 Z. Qin, D. Li, Y. Lan, Q. Li and R. Yang, *Ind. Eng. Chem. Res.*, 2015, **54**, 10707–10713.

17 J. C. Liu, M. J. Xu, T. Lai and B. Li, *Ind. Eng. Chem. Res.*, 2015, **54**, 9733–9741.

18 S. Duquesne, M. Le Bras, S. Bourbigot, R. Delobel, G. Camino, B. Eling, C. Lindsay, T. Roels and H. Vezin, *J. Appl. Polym. Sci.*, 2001, **82**, 3262–3274.

19 Y. Shi, Z. Gui, B. Yuan, Y. Hu and Y. Zheng, *J. Therm. Anal. Calorim.*, 2018, **131**, 1067–1077.

20 Y. Zhang, B. Wang, B. Yuan, Y. Yuan, K. M. Liew, L. Song and Y. Hu, *Ind. Eng. Chem. Res.*, 2017, **56**, 7468–7477.

21 F. Carosio, J. Alongi and G. Malucelli, *Carbohydr. Polym.*, 2012, **88**, 1460–1469.

22 T. Van Truong and D. J. Kim, *Environ. Res.*, 2022, **212**, 113448.

23 X. He, J. Sun, X. Xu, Z. Lv and J. Song, *J. Therm. Anal. Calorim.*, 2017, **130**, 2249–2255.

24 M. K. Naskar and M. Chatterjee, *J. Am. Ceram. Soc.*, 2005, **88**, 3322–3326.

25 W. Liu and H. Zuo, *J. Non-Cryst. Solids*, 2021, **567**, 120940.